Biochemistry and Biophysics Reports 5 (2016) 396–400

Contents lists available at ScienceDirect

Biochemistry and Biophysics Reports

journal homepage: www.elsevier.com/locate/bbrep

Isothermal titration calorimetry uncovers substrate promiscuity of bicupin oxalate oxidase from *Ceriporiopsis subvermispora*

Hassan Rana [a], Patricia Moussatche [b], Lis Souza Rocha [a], Sofiene Abdellaoui [c], Shelley D. Minteer [c], Ellen W. Moomaw [a,*]

[a] Department of Chemistry and Biochemistry, Kennesaw State University, Kennesaw, GA 30144, USA
[b] Foundation for Applied Molecular Evolution Alachua, FL 32615, USA
[c] Department of Chemistry, University of Utah, Salt Lake City, UT 84112, USA

ARTICLE INFO

Article history:
Received 30 September 2015
Received in revised form
30 December 2015
Accepted 28 January 2016
Available online 4 February 2016

Keywords:
Oxalate oxidase
Isothermal titration calorimetry
Enzyme kinetics
Cupin

ABSTRACT

Isothermal titration calorimetry (ITC) may be used to determine the kinetic parameters of enzyme-catalyzed reactions when neither products nor reactants are spectrophotometrically visible and when the reaction products are unknown. We report here the use of the multiple injection method of ITC to characterize the catalytic properties of oxalate oxidase (OxOx) from *Ceriporiopsis subvermispora* (CsOx-Ox), a manganese dependent enzyme that catalyzes the oxygen-dependent oxidation of oxalate to carbon dioxide in a reaction coupled with the formation of hydrogen peroxide. CsOxOx is the first bicupin enzyme identified that catalyzes this reaction. The multiple injection ITC method of measuring OxOx activity involves continuous, real-time detection of the amount of heat generated (dQ) during catalysis, which is equal to the number of moles of product produced times the enthalpy of the reaction (ΔH_{app}). Steady-state kinetic constants using oxalate as the substrate determined by multiple injection ITC are comparable to those obtained by a continuous spectrophotometric assay in which H_2O_2 production is coupled to the horseradish peroxidase-catalyzed oxidation of 2,2′-azinobis-(3-ethylbenzthiazoline-6-sulfonic acid) and by membrane inlet mass spectrometry. Additionally, we used multiple injection ITC to identify mesoxalate as a substrate for the CsOxOx-catalyzed reaction, with a kinetic parameters comparable to that of oxalate, and to identify a number of small molecule carboxylic acid compounds that also serve as substrates for the enzyme.

1. Introduction

Cereporiopsis subvermispora is a white rot basidiomycete fungus that efficiently depolymerizes lignin [1] and is of interest in degrading biomass for the production of ethanol [2], sugar [3], and methane [4]. Oxalate oxidase (OxOx) catalyzes the cleavage of the carbon–carbon bond of oxalate to yield two moles of carbon dioxide as dioxygen is reduced to hydrogen peroxide [5]. While not fully understood, the role of oxalate oxidase in *C. subvermispora* (CsOxOx) has been proposed to provide a source of extracellular hydrogen peroxide for manganese peroxidase to oxidize Mn^{2+} to Mn^{3+} [6, 7], which is a robust and diffusible oxidant able to degrade many components of lignin [8]. Oxalate oxidase activity has been found in a number plant species including rice [9], wheat [10], barley [11,12,13], beet [14,15], and sorghum [16,17] where it has been shown to play roles in signaling and in the defense against pathogenic microbes [18]. Plant OxOx enzymes possess a single cupin (β-barrel) domain containing a single manganese ion and are, therefore, structurally characterized and classified as monocupins [19,20,21,22]. Sequence analysis indicates that CsOxOx is the first manganese-containing bicupin enzyme identified that catalyzes the oxidation of oxalate [23,24,25].

Oxalate oxidase is of commercial interest for a number of applications including the determination of oxalate levels in blood and urine [26,27], the protection of plants against pathogens, the production of transgenic plants with reduced levels of oxalate [19,28], pulping in the paper industry [19,29,30,31], and as a component of enzymatic biofuel cells [32,33]. The utility of OxOx as a biocatalyst for anodic electrode reactions in biofuel cells motivates efforts to tailor the properties of the enzyme to this application through directed evolution and/or rational design [34,35]. Understanding the degree of promiscuity (or fidelity) of CsOxOx is an important

Abbreviations: OxOx, oxalate oxidase; CsOxOx, OxOx from *Ceriporiopsis subvermispora*; HRP, horseradish peroxidase; ABTS, 2,2′-azinobis-(3-ethylbenzthiazoline-6-sulfonic acid).

* Corresponding author.
E-mail address: emoomaw@kennesaw.edu (E.W. Moomaw).

http://dx.doi.org/10.1016/j.bbrep.2016.01.016

endeavor as it may provide a basis for these modifications. Previous enzymatic characterization of CsOxOx employing a continuous spectrophotometric assay in which H_2O_2 production is coupled to the horseradish peroxidase (HRP) catalyzed oxidation of 2,2′-azinobis-(3-ethylbenzthiazoline-6-sulfonic acid) (ABTS) determined that acetate and other small molecule carboxylic acid compounds (malonate, malate, glycolate, glyoxylate, and pyruvate) reduced the rate of oxalate oxidation at low concentrations of oxalate. Uninhibited maximal reaction rates could, however, be achieved at high substrate concentrations, suggesting that these molecules were competitive inhibitors [24]. Using the HRP coupled assay, none of these molecules served as substrates.

Isothermal titration calorimetry (ITC) may be used to determine the kinetic parameters of enzyme catalyzed reactions even if the identity of the products are not known [36,37,38]. The multiple injection ITC method of measuring OxOx activity involves continuous, real-time detection of the amount of heat generated (dQ) during catalysis, which is equal to the number of moles of product produced times the enthalpy of the reaction (ΔH_{app}). Determination of the kinetic parameters of a reaction using this method, therefore, requires two experiments 1) determination of the enthalpy of the reaction from the complete conversion of substrate to product, and 2) determination of the differential power effects from the continuous conversion of substrate to product. We report here the use of ITC to characterize the catalytic properties of oxalate oxidase through the direct and continuous detection of the amount of heat generated. Furthermore, we used multiple injection ITC to identify mesoxalate (oxopropanedioic acid) as a substrate for CsOxOx with a kinetic parameters comparable to that of oxalate and to identify other small molecule carboxylic acids (that were previously shown to be competitive inhibitors) as substrates for CsOxOx.

2. Materials and methods

2.1. Materials

Recombinant oxalate oxidase from *C. subvermispora* was expressed and purified as a secreted soluble protein using a *Pichia pastoris* expression system as previously described [24].

Reagents were of the highest purity available and were purchased from either Sigma-Aldrich or Fisher Scientific unless otherwise stated. A modified Lowry assay (Pierce) was used to determine protein concentration using bovine serum albumin as a standard [39].

2.2. Coupled steady-state kinetic assay

The oxalate oxidase-catalyzed oxidation of oxalate was measured using a continuous, coupled spectrophotometric assay in which the formation of hydrogen peroxide is coupled to the HRP-catalyzed oxidation of 2,2′-azinobis-(3-ethylbenzthiazoline-6-sulfonic acid) (ABTS) [13]. Each assay contained 25 U HRP, 5 mM ABTS, 50 mM potassium oxalate, and 1 μM CsOxOx dissolved in the indicated buffer, pH 4.0 (total volume 1.0 mL) and was monitored at 650 nm. An extinction coefficient of 10,000 M^{-1} cm^{-1} for the ABTS radical product was used in the rate calculations. Control samples without HRP were carried out in order to distinguish between H_2O_2 production and any oxalate-dependent dye oxidation activity by CsOxOx. Reactions were carried out at specific substrate and enzyme concentrations in duplicate, and data were analyzed to obtain the values of V_{max} and V_{max}/K_m by standard computer-based methods [40].

2.3. Isothermal titration calorimetry

Calorimetric measurements were performed using a Nano ITC Low Volume (TA Instruments) equipped with a 24 K gold reaction cell (190 μL volume). Degassed solutions were equilibrated at 25.0 °C with stirring at 125 rpm. A 50 μL stirred syringe inserted into a buret handle was used to inject substrate into the sample cell. Water was used in the reference cell. Heat (Q) produced from the chemical reaction between enzyme and substrate was measured by the continuous supply of instrumental thermal power (dQ/dt) to the sample cell, which maintains isothermal condition between the sample cell and reference cell. Thermal power relates to enzyme reaction rate:

$$\frac{dQ}{dt} = \frac{d[P]}{dt} \times V \times \Delta H \quad (1)$$

where V is the volume of the solution in the sample cell, ΔH is the apparent enthalpy, and $(d[P])/dt$ is the enzyme reaction rate. When Eq. (1) is solved for $(d[P])/dt$, the resulting equation is:

$$\frac{d[P]}{dt} = \frac{1}{V \times \Delta H} \times \frac{d[Q]}{dt} \quad (2)$$

Protein samples were exhaustively dialyzed into the reaction buffer (25 mM sodium succinate, pH 4.0) and substrate solutions were prepared in the resulting dialysate. Enzyme concentrations for the rate determinations ranged from 112 nm to 456 nM as described in the Two blank reactions were performed for each condition tested: 1) the injection of substrate into buffer and 2) the injection of buffer into enzyme solution. These blank heat effects were subtracted to yield the corrected heat rate of reaction. NanoAnalyze (TA Instruments Inc.) was used to transform the raw ITC data into reaction rates according to Eqs. (1) and (2) above and to obtain the values of k_{cat} and K_m. The instrument is an overflow calorimeter and the volume, therefore remains constant, but the number of moles does change as volume is displaced. This is tracked in the NanoAnalyze software.

2.4. Calorimetric determination enthalpies of reaction

The apparent molar enthalpies of oxalate and other possible substrates were determined by measuring the power required to maintain constant temperature in conditions where the reaction proceeded to completion. These conditions required the use of higher enzyme concentrations (1 μM) and lower substrate concentrations (2 mM) than the corresponding rate determination experiments. Upon complete consumption of substrate, the power returned to baseline. The experimental enthalpy relates to the area under the curve (less the blank heat of the mixing event) according to Eq. (3).

$$\Delta H_{app} = \frac{1}{[S]*V} \int_{t=0}^{t=\infty} \frac{dQ(t)}{dt} dt \quad (3)$$

3. Results and discussion

3.1. Direct detection of CsOxOx activity

Direct measurement of enzymatic reaction rates has numerous advantages over a coupled assay. Previously, we reported the use of membrane inlet mass spectrometry (MIMS) as a direct and continuous method to measure oxalate oxidase activity [41]. In the MIMS assay method, ^{13}C doubly labeled oxalate is used to distinguish the CO_2 generated by CsOxOx from adventitious CO_2 dissolved in the reaction mixtures. Since the use of labeled substrates

places constraints of expense and availability on the molecules tested for activity as substrates, we investigated the applicability of the multiple injection method of isothermal titration calorimetry for the direct detection of the CsOxOx-catalyzed oxidation of oxalate.

The steady-state kinetic parameters of CsOxOx are sensitive to the buffer in the reaction mixture [24]. Steady-state measurements using the coupled assay carried out in acetate buffer, pH 4.0 resulted in a V_{max} value of 21.2 U/mg, which compares favorably with the value obtained for the native enzyme [42]. The K_m for oxalate, measured in acetate buffer, however, is 14.9 mM, which is significantly higher than the 0.1 mM value reported for the native enzyme. Succinate buffer, pH 4.0 yields a K_m value for oxalate of 1.5 mM while citrate buffer, pH 4.0 yields a K_m of 0.1 mM. The V_{max} in citrate is, however, reduced (V_{max}=8.1 U/mg) and the addition of succinate increases the activity of the citrate-inhibited enzyme [24]. These results suggest that citrate may be an uncompetitive inhibitor. Succinate appears to displace citrate without inhibiting the enzyme. There is no evidence for succinate inhibition. Using these conditions, we determined the apparent enthalpy of the CsOxOx reaction by measuring the amount of heat exchanged during the complete conversion of substrate into product. A typical calorimetric trace (heat flow as a function of time) is shown in Fig. 1. The 180 μL reaction containing 1 μM CsOxOx was allowed to reach thermal equilibrium at 25 °C before beginning the experiment. The baseline was collected for 1 min then the reaction was initiated by the addition of oxalate (prepared in the enzyme dialysate) to a final concentration of 10 μM. The response time of the instrument was observed to be about 18 s, after which the thermal power generated by the enzyme registered as offsetting instrumental thermal power. The instrumental default setting of plotting exothermic events in the upward direction was left intact. After the complete consumption of the substrate, the power returned to the original baseline. Four hundred seconds after the first injection, a second identical injection was made into the same reaction mixture (now containing product), which resulted in a calorimetric trace almost identical in area and shape. A blank titration of oxalate into buffer was collected (data not shown) and its heat was subtracted from that of the substrate into enzyme titration, resulting in an experimental ΔH_{app} value of -5.6 ± 0.3 kJ/mol (uncertainty represents curve fitting errors).

3.2. Steady-state kinetic characterization of the CsOxOx catalyzed reaction by ITC

The differential power effects from the continuous conversion

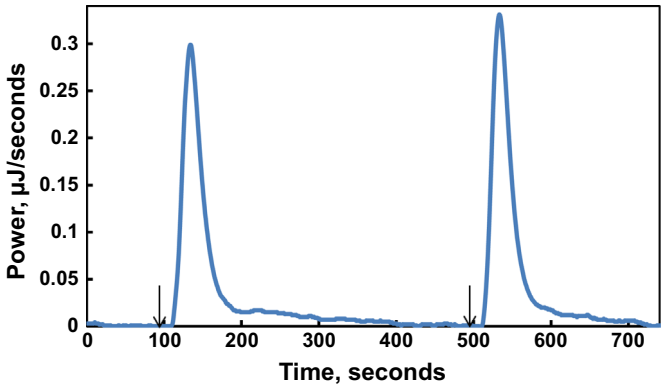

Fig. 1. Heat flow as a function of time for the CsOxOx-catalyzed complete conversion of oxalate into products gives the ΔH_{app} of reaction. After equilibration at 25 °C (not shown), the reaction was initiated by the addition of 1 μL of 2 mM potassium oxalate, pH 4.0 into 1 μM CsOxOx (180 μL) in 50 mM sodium succinate, pH 4.0 (first arrow). This injection was repeated at 500 s (second arrow).

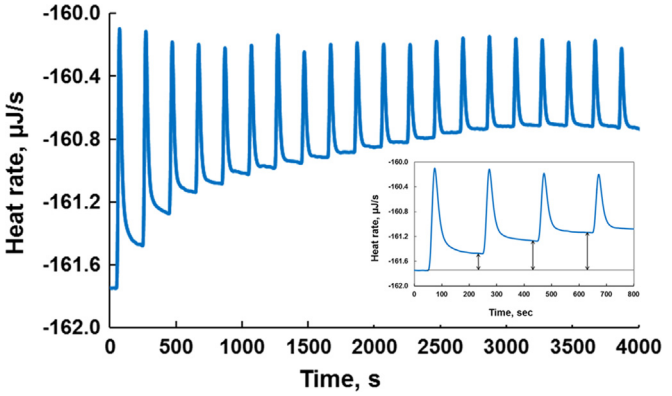

Fig. 2. Thermogram monitoring the power required to maintain isothermal conditions of 20 successive injections of 2 μL of 20 mM oxalate into 112 nM oxalate oxidase (180 μL) previously thermally equilibrated at 25 °C. Under these conditions, when the enzyme velocity reaches a new steady state, the power remains constant. The inset corresponds to the first four injections of substrate into the sample cell and the arrows represent the decrease in the heat flow (dQ/dt) required to maintain thermal equilibrium at each steady state condition.

of oxalate to carbon dioxide and hydrogen peroxide is shown in Fig. 2. After thermal equilibration, injections of oxalate were made every 200 s into a solution originally 114 nM CsOxOx, resulting in final oxalate concentrations ranging from 0.200 mM to 3.700 mM (due to volume displacement). The rate of the uncatalyzed reaction is negligible and the plateaus reached between injections indicate that at each new concentration of substrate a new constant [ES] is achieved. The inset in Fig. 2 shows the first four injections of oxalate into the sample cell and the arrows represent the decrease in the instrumental power required at each equilibrium condition (dQ_1/dt, dQ_2/dt, and dQ_3/t). The Michaelis–Menten equation was used to fit these data (Fig. 3). The set in Fig. 3 displays the same data in a Lineweaver–Burk plot. The kinetic parameters are shown in Table 1 along with those determined by the membrane inlet mass spectrometry assay [41] and the horse radish peroxidase coupled assay [24]. There is good agreement among the three methods.

3.3. Mesoxalate is a substrate for CsOxOx with kinetic parameters comparable to those of oxalate

Given the interest in oxalate oxidase as a component of enzymatic biofuel cells [32,33], we tested the ability of CsOxOx to catalyze a reaction using mesoxalate as the substrate. A typical heat flow versus time plot for the reaction catalyzed by CsOxOx

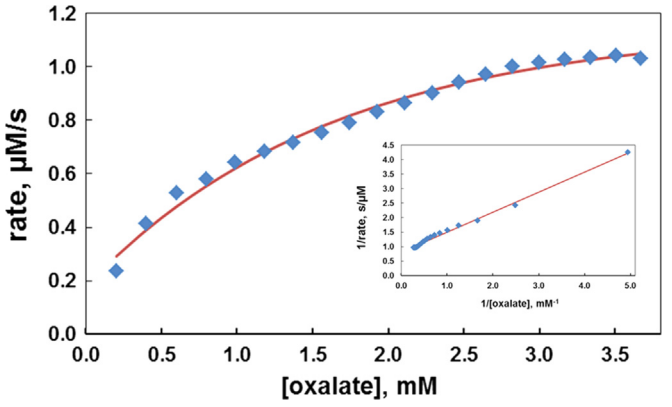

Fig. 3. Rate versus oxalate concentration data from Fig. 2 fitted to the Michaelis–Menten equation to give kinetic parameters provided in Table 1. The inset shows the same data in a double reciprocal plot yielding the nearly identical values of k_{cat} and K_m as the fit to the Michaelis–Menten equation.

Table 1
Steady-state kinetic parameters for the CsOxOx-catalyzed oxidation of oxalate measured by ITC, membrane inlet mass spectrometry, and the horse radish peroxidase coupled assay. Uncertainties represent standard errors in the fit to the Michaelis–Menten expression.

Assay	K_m (oxalate), mM	k_{cat}, s^{-1}	k_{cat}/K_m, mM^{-1} s^{-1}
ITC	**0.86 ± 0.1**	**15.6 ± 0.3**	**18.0 ± 0.3**
MIMS[a]	**0.93 ± 0.1**	**22.3 ± 0.3**	**24.0 ± 0.4**
ABTS[b]	**1.5 ± 0.1**	**20.0 ± 0.4**	**13.3 ± 0.4**

[a] Data previously reported in [41].
[b] Data previously reported in [24].

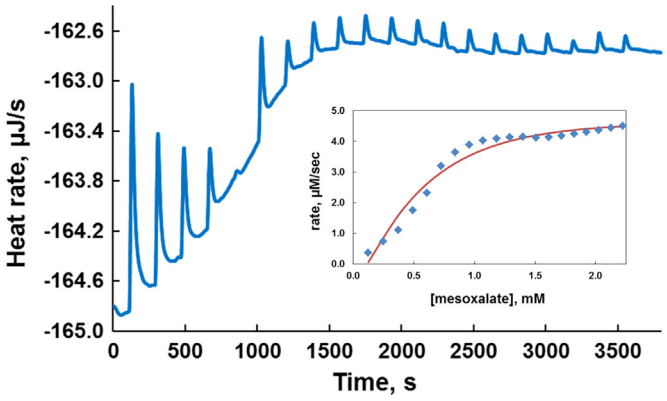

Fig. 4. The heat flow as a function of time for the reaction catalyzed by CsOxOx using mesoxalate as substrate measured in conditions of steady-state kinetics at 25 °C. The sample cell contained 180 µL of 456 nM CsOxOx and 20 injections of 2.5 µL of 10 mM mesoxalate were performed with an interval of 180 s between them. The inset shows the rate versus mesoxalate concentration data fitted to the Michaelis–Menten equation to give kinetic parameters provided in Table 2 for mesoxalate.

Table 2
Steady-state kinetic parameters for the CsOxOx- catalyzed oxidation of alternative substrates measured by ITC. Uncertainties represent standard errors in the fit to the Michaelis–Menten expression.

Substrate	K_m, mM	k_{cat}, s^{-1}	Relative activity[a], %
Oxalate	**0.86 ± 0.1**	**15.6 ± 0.3**	**100**
Mesoxalate	**0.52 ± 0.1**	**9.9 ± 0.3**	**63.5**
Glyoxalate	**7.10 ± 0.1**	**0.46 ± 0.1**	**2.9**
Malonate	**6.42 ± 0.1**	**3.21 ± 0.1**	**20.5**
Pyruvate	**2.89 ± 0.1**	**1.25 ± 0.1**	**8.0**
Malate	**−nd**[b]	**nd**[b]	**< 0.01**

[a] Activity relative to that with oxalate in 50 mM sodium succinate, pH 4.0.
[b] Values were too low to be determined.

using mesoxalate as substrate under steady-state kinetics is shown in Fig. 4. In the experiment shown, the sample cell contained 180 µL of 456 nM CsOxOx and 20 injections of 2.5 µL of 10 mM mesoxalate (final concentrations ranged from 0.125 to 2.224 mM) were performed with an interval of 180 s between them. Although the shape of the data was not an ideal rectangular hyperbola, the steady state data was fit to the Michaelis–Menten equation (inset) and converted to a rate by the enthalpy of reaction. The kinetic parameters obtained are reproducible, the observed anomalies between the data and the Michaelis–Menten fits, however, vary due to the small heat changes being measured and because the quality of the data depends of factors such as movement in the lab and slight electrical changes due to nearby equipment switching cycles. Our best ITC data is often collected when these disturbances are minimized such as evening and weekends. The heat flow as a function of time for the CsOxOx-catalyzed complete conversion of mesoxalate into product to determine the ΔH_{app} of reaction (−3.1 kJ/mol) is presented as Supplementary Fig 1. The $K_m = 0.52 \pm 0.1$ mM for the reaction using mesoxalate, which is slightly lower than for the reaction using oxalate (Table 2). The $k_{cat} = 9.9 \pm 0.3$ s^{-1}, which is two thirds of the rate using oxalate as determined by ITC. The ABTS dye oxidation assay results in a 20-fold lower k_{cat} value (0.5 s^{-1}) and a K_m value of 29 mM (data not shown). We propose that the predominant products of the CsOxOx-catalyzed reaction of mesoxalate are glyoxalic acid and carbon dioxide, making this reaction transparent in the ABTS assay. We have used membrane inlet mass spectrometry to detect carbon dioxide formation (data not shown) but are unable to quantify the rate without ^{13}C labeled mesoxalate, which is currently prohibitively expensive. In pondering why a secreted enzyme of a white rot fungus would use mesoxalate as a substrate, we found that the common reed (*Phragmites australis*) secretes gallic acid, which is photodegraded into mesoxalate in order to ward off encroaching plants [43].

3.4. CsOxOx is a promiscuous enzyme

The observation that mesoxalate serves as a substrate for the CsOxOx-catalyzed reaction prompted the reevaluation of molecules that had previously been shown to be competitive inhibitors using the spectrophotometric ABTS assay [24]. Table 2 shows the kinetic parameters of glyoxalate, pyruvate, and malonate determined by measuring thermal power compensation during turnover using the ITC (Supplementary information). Malate does not serve as a substrate for CsOxOx using this method (data not shown). These results reveal that CsOxOx possesses a much higher degree of substrate promiscuity than was previously thought. Future work to understand the amino acid residues involved in this promiscuity may provide insight into the evolutionary route CsOxOx has traveled and inform a path toward its modification for its use in the oxidation of fuel molecules in enzymatic cells.

In summary, we have demonstrated the use of ITC provides a sensitive assay for oxalate oxidase and we have used this technique to reveal that CsOxOx uses mesoxalate with kinetic parameters comparable to those for oxalate. Additionally, we have shown that CsOxOx uses a variety of small molecule carboxylic acids as substrates. We anticipate that this technique will find broad application in the field of bioelectrocatalysis where, because of dye interactions with redox enzymes, dye-based spectroscopic assays frequently show different behavior than electrode based assays.

Acknowledgments

We are grateful to Dr. Jonathan McMurry (Kennesaw State University) for the use of the isothermal titration calorimeter and to Dr. Colette Quinn (TA Instruments) for her reading of this manuscript. This work was supported by the National Science Foundation (MCB-1041912) to EWM and by the Office of the Vice President of Reasearch (Kennesaw State University).

Appendix A. Transparency Document

Transparency Document associated with this article can be found in the online version at http://dx.doi.org/10.1016/j.bbrep.2016.01.016.

References

[1] M.R. Makela, N. Donofrio, R.P. de Vries, Plant biomass degradation by fungi, Fungal Genet. Biol. 72 (2014) 2–9.
[2] R.L. Giles, J.C. Zackeru, E.R. Galloway, G.D. Elliott, M.W. Parrow, Single versus simultaneous species treatment of wood with *Ceriporiopsis subvermispora* and *Postia placenta* for ethanol applications, with observations on interspecific growth inhibition, Int. Biodeterior. Biodegrad. 99 (2015) 66–72.
[3] S. Cianchetta, B. Di Maggio, P.L. Burzi, S. Galletti, Evaluation of selected white-rot fungal isolates for improving the sugar yield from wheat straw, Appl. Biochem. Biotechnol. 173 (2014) 609–623.
[4] J. Zhao, X.M. Ge, J. Vasco-Correa, Y.B. Li, Fungal pretreatment of unsterilized yard trimmings for enhanced methane production by solid-state anaerobic digestion, Bioresour. Technol. 158 (2014) 248–252.
[5] H. Shimazono, Oxalic acid decarboxylase, a new enzyme from the mycelium of wood destroying fungi, J. Biochem. 42 (1955) 321–340.
[6] U. Urzua, P.J. Kersten, R. Vicuna, Kinetics of Mn3+-oxalate formation and decay in reactions catalyzed by manganese peroxidase of Ceriporiopsis subvermispora, Arch. Biochem. Biophys. 360 (1998) 215–222.
[7] U. Urzua, P.J. Kersten, R. Vicuna, Manganese peroxidase dependent oxidation of glyoxylic and oxalic acids synthesized by *Ceriporiopsis subvermispora* produces extracellular hydrogen peroxide, Appl. Environ. Microbiol. 64 (1998) 68–73.
[8] K.A. Jensen, W. Bao, S. Kawai, E. Srebotnik, K.E. Hammel, Manganese-dependent cleavage of nonphenolic lignin structures by *Ceriporiopsis subvermispora* in the absence of lignin peroxidase, Appl. Environ. Microbiol. 62 (1996) 3679–3686.
[9] M.C. Carrillo, P.H. Goodwin, J.E. Leach, H. Leung, C.M.V. Cruz, Phylogeny, function and structure of rice oxalate oxidases, Phytopathology 98 (2008), S31-S31.
[10] J.M. Dunwell, Cupins: a new superfamily of functionally diverse proteins that include germins and plant storage proteins, Biotechnol. Genet. Eng. Rev. 15 (1998) 1–32.
[11] V.P. Kotsira, Y.D. Clonis, Oxalate oxidase from barley roots: purification to homogeneity and study of some molecular, catalytic, and binding properties, Arch. Biochem. Biophys. 340 (1997) 239–249.
[12] J. Chiriboga, Purification and properties of oxalic acid oxidase, Arch. Biochem. Biophys. 116 (1966) 516–523.
[13] L. Requena, S. Bornemann, Barley (*Hordeum vulgare*) oxalate oxidase is a manganese-containing enzyme, Biochem. J. 343 (Pt 1) (1999) 185–190.
[14] P. Varalakshmi, K.E. Richardson, Studies on oxalate oxidase from beet stems upon immobilization on concanavalin A, Biochem. Int. 26 (1992) 153–162.
[15] A.E. Leek, V.S. Butt, Oxidation of oxalate and formate by leaf peroxisomes, Biochem. J. 128 (1972) 87P.
[16] Satyapal, C.S. Pundir, Purification and properties of an oxalate oxidase from leaves of grain sorghum hybrid CSH-5, Biochim. Biophys. Acta 1161 (1993) 1–5.
[17] C.S. Pundir, N.K. Kuchhal, Satyapal, Barley oxalate oxidase immobilized on zirconia-coated alkylamine glass using glutaraldehyde, Indian J. Biochem. Biophys. 30 (1993) 54–57.
[18] B.G. Lane, Oxalate oxidases and differentiating surface structure in wheat: germins, Biochem. J. 349 (2000) 309–321.
[19] J.M. Dunwell, S. Khuri, P.J. Gane, Microbial relatives of the seed storage proteins of higher plants: conservation of structure and diversification of function during evolution of the cupin superfamily, Microbiol. Mol. Biol. Rev. 64 (2000) 153–179.
[20] J.M. Dunwell, A. Purvis, S. Khuri, Cupins: the most functionally diverse protein superfamily? Phytochemistry 65 (2004) 7–17.
[21] J.M. Dunwell, P.J. Gane, Microbial relatives of seed storage proteins: conservation of motifs in a functionally diverse superfamily of enzymes, J. Mol. Evol. 46 (1998) 147–154.
[22] J.M. Dunwell, A. Culham, C.E. Carter, C.R. Sosa-Aguirre, P.W. Goodenough, Evolution of functional diversity in the cupin superfamily, Trends Biochem. Sci. 26 (2001) 740–746.
[23] M.R. Escutia, L. Bowater, A. Edwards, A.R. Bottrill, M.R. Burrell, R. Polanco, R. Vicuna, S. Bornemann, Cloning and sequencing of two *Ceriporiopsis subvermispora* bicupin oxalate oxidase allelic isoforms: implications for the reaction specificity of oxalate oxidases and decarboxylases, Appl. Environ. Microbiol. 71 (2005) 3608–3616.
[24] P. Moussatche, A. Angerhofer, W. Imaram, E. Hoffer, K. Uberto, C. Brooks, C. Bruce, D. Sledge, N.G. Richards, E.W. Moomaw, Characterization of *Ceriporiopsis subvermispora* bicupin oxalate oxidase expressed in *Pichia pastoris*, Arch. Biochem. Biophys. 509 (2011) 100–107.
[25] E.W. Moomaw, E. Hoffer, P. Moussatche, J.C. Salerno, M. Grant, B. Immelman, R. Uberto, A. Ozarowski, A. Angerhofer, Kinetic and spectroscopic studies of bicupin oxalate oxidase and putative active site mutants, PLoS One 8 (2013) e57933.
[26] A. Hesse, D. Bongartz, H. Heynck, W. Berg, Measurement of urinary oxalic acid: a comparison of five methods, Clin. Biochem. 29 (1996) 467–472.
[27] R. Honow, D. Bongartz, A. Hesse, An improved HPLC-enzyme-reactor method for the determination of oxalic acid in complex matrices, Clin. Chim. Acta 261 (1997) 131–139.
[28] C. Thompson, J.M. Dunwell, C.E. Johnstone, V. Lay, J. Ray, H. Schmitt, H. Watson, G. Nisbet, Degradation of oxalic acid by trangenic oilsee rape plants expressing oxalate oxidase, Euphytica 85 (1995) 169–172.
[29] Y. Wei, Z. Zhang, C.H. Andersen, E. Schmelzer, P.L. Gregersen, D.B. Collinge, V. Smedegaard-Petersen, H. Thordal-Christensen, An epidermis/papilla-specific oxalate oxidase-like protein in the defence response of barley attacked by the powdery mildew fungus, Plant Mol. Biol. 36 (1998) 101–112.
[30] H. Strasser, W. Burgstaller, F. Schinner, High-yield production of oxalic acid for metal leaching processes by *Aspergillus niger*, FEMS Microbiol. Lett. 119 (1994) 365–370.
[31] C. Ruttimann-Johnson, L. Salas, R. Vicuna, T.K. Kirk, Extracellular enzyme production and synthetic lignin mineralization by *Ceriporiopsis subvermispora*, Appl. Environ. Microbiol. 59 (1993) 1792–1797.
[32] D.P. Hickey, M.S. McCammant, F. Giroud, M.S. Sigman, S.D. Minteer, Hybrid enzymatic and organic electrocatalytic cascade for the complete oxidation of glycerol, J. Am. Chem. Soc. 136 (2014) 15917–15920.
[33] S. Xu, S.D. Minteer, Enzymatic biofuel cell for oxidation of glucose to CO_2, ACS Catal. 2 (2012) 91–94.
[34] V. Balland, C. Hureau, A.M. Cusano, Y. Liu, T. Tron, B. Limoges, Oriented immobilization of a fully active monolayer of histidine-tagged recombinant laccase on modified gold electrodes, Chemistry 14 (2008) 7186–7192.
[35] O. Spadiut, I. Pisanelli, T. Maischberger, C. Peterbauer, L. Gorton, P. Chaiyen, D. Haltrich, Engineering of pyranose 2-oxidase: improvement for biofuel cell and food applications through semi-rational protein design, J. Biotechnol. 139 (2009) 250–257.
[36] M.J. Todd, J. Gomez, Enzyme kinetics determined using calorimetry: a general assay for enzyme activity? Anal. Biochem. 296 (2001) 179–187.
[37] M.L. Bianconi, Calorimetry of enzyme-catalyzed reactions, Biophys. Chem. 126 (2007) 59–64.
[38] K. Maximova, J. Trylska, Kinetics of trypsin-catalyzed hydrolysis determined by isothermal titration calorimetry, Anal. Biochem. 486 (2015) 24–34.
[39] O.H. Lowry, N.J. Rosebrough, A.L. Farr, R.J. Randall, Protein measurement with the Folin phenol reagent, J. Biol. Chem. 193 (1951) 265–275.
[40] W.W. Cleland, Statistical analysis of enzyme kinetic data, Methods Enzymol. 62 (1979) 151–160.
[41] E.W. Moomaw, R. Uberto, C. Tu, Membrane inlet mass spectrometry reveals that *Ceriporiopsis subvermispora* bicupin oxalate oxidase is inhibited by nitric oxide, Biochem. Biophys. Res. Commun. 450 (2014) 750–754.
[42] C. Aguilar, U. Urzua, C. Koenig, R. Vicuna, Oxalate oxidase from *Ceriporiopsis subvermispora*: biochemical and cytochemical studies, Arch. Biochem. Biophys. 366 (1999) 275–282.
[43] T. Rudrappa, Y.S. Choi, D.F. Levia, D.R. Legates, K.H. Lee, H.P. Bais, Phragmites australis root secreted phytotoxin undergoes photo-degradation to execute severe phytotoxicity, Plant Signal. Behav. 4 (2009) 506–513.